

## MOLECULAR CLOUDS ASSOCIATED WITH H I SHELLS

B-C. Koo and C. Heiles

Astronomy Department, University of California, Berkeley,  
Berkeley, California U.S.A.

**Abstract:** We report the detection of molecular clouds associated with three giant galactic H I shells.

**Introduction:** The interstellar H I is concentrated into shells and filaments with diameters ranging up to more than a hundred degrees, which are believed to be formed by stellar winds and/or supernovae, or by the collision of high velocity clouds with the galactic disk (Heiles 1984 and references therein). In any case, the shell represents the gas piled up by the interstellar shock waves. This cool and relatively dense region will be one of the good birth places for molecular clouds and therefore stars.

In this paper, we report the detection of molecular clouds in three giant H I shells (Heiles 1984): GS 090-28-17, GS 135+29+4, and GS 193-32+4. We carried out CO observations using the 6 m telescopes of the Hat Creek Observatory during the scattered period from 1986 to 1987. Initial observations were made along the line segments crossing the local maximum of H I emission features in well-isolated portions of each shell. For GS 090-28-17 and GS 135+29+4, small areas ( $\sim 1^\circ \times 1^\circ$ ) around the initial detection have been mapped with a rms noise level of 0.3 K. Also, the  $^{13}\text{CO}$  (J=1-0) line was observed for several points which have shown strong  $^{12}\text{CO}$  emission.

**H I Shells and Molecular Clouds:** The large scale structures of the H I shells are exhibited by their H I distributions in Figure 1, where the positions of the detected molecular clouds are also shown by triangles. The H I maps are obtained by integrating the H I survey data of Heiles and Habing (1974) over the velocity interval of the H I shells. The resulting H I distributions are represented by gray scale maps superposed on the contour maps; areas with larger column densities are blacker.

Two shells, GS 090-28-17 and GS 135+29+4, show almost complete loop structures in the H I distribution. In GS 135+29+4, the velocity at the peak intensity increases from 0 to  $7 \text{ km s}^{-1}$  as we move from both ends of the loop towards  $(l,b)=(127,39)$ . This is the velocity gradient expected for an expanding loop with  $\sim 7 \text{ km s}^{-1}$  when we are looking at parts of it moving away from us. The large shell GS 190-32-4, which is also known as the Eridanus loop, is one of the best examples that show the velocity structure of expanding shell (Heiles 1976). Around our observed position in GS 190-32-4, we see complex filamentary structures. Some of the filaments are parts of another large shell GS 120-30-8, which has diameter of 100 degrees.

The velocities of the detected molecular clouds agree with H I shell velocities in all cases: CO velocity ranges from  $-17$  to  $-13$   $\text{km s}^{-1}$  in GS 090-28-17,  $0$  to  $3$   $\text{km s}^{-1}$  in GS 135+29+4, and  $-7$  to  $-4$   $\text{km s}^{-1}$  and  $2$  to  $5$   $\text{km s}^{-1}$  in GS 193-32+4. (Two clouds with velocities different from each other by  $10$   $\text{km s}^{-1}$  were detected in GS 193-32+4.) The coincidence of velocities and positions between molecular clouds and H I shells strongly suggests that they are physically associated with each other. In GS 190-32+4, however, the complex filamentary structure prevents us from associating molecular clouds with H I shells.

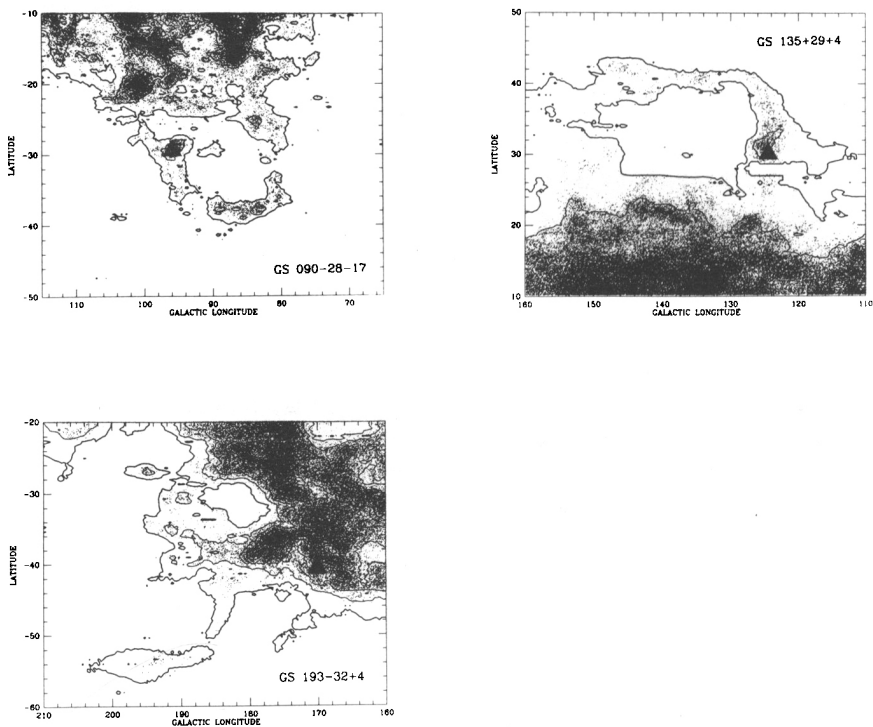


Figure 1. Large scale structures of three giant H I shells are exhibited by their H I distributions. Also, the positions of the detected molecular clouds are shown by triangles. The H I distributions are obtained by integrating over velocities from  $-22$  to  $-13$   $\text{km s}^{-1}$  for GS 090-28-17,  $-4$  to  $13$   $\text{km s}^{-1}$  for GS 135+29+4, and  $-6$  to  $5$   $\text{km s}^{-1}$  for GS 193-32-4. The contour level increases from  $30$  to  $110$   $\text{K km s}^{-1}$  by increments of  $20$   $\text{K km s}^{-1}$  for GS 090-28-17,  $100$  to  $400$   $\text{K km s}^{-1}$  by  $100$   $\text{K km s}^{-1}$  for GS 135+29+4, and  $100$  to  $300$   $\text{K km s}^{-1}$  by  $50$   $\text{K km s}^{-1}$  for GS 193-32+4. Areas with larger column densities are blacker.

Figure 2 shows integrated CO contour maps of the molecular clouds detected in GS 090-28-17 and GS 135+29+4. The beam spacing is  $\sim 6'$ , which is three times the beam size. The molecular clouds in GS 090-28-17 have sizes ranging from a few minutes of arc to a few tens of minutes of arc. The molecular clouds in GS 135+29+4 are bigger than  $1^\circ$  and the observations did not cover the whole cloud. The observed ratio  $T_A^+(^{12}\text{CO})/T_A^+(^{13}\text{CO})$  ranges from 5 to 15 and implies that CO is optically thick.

**Molecular clouds in GS 090-28-17:** The mapping is almost complete for two molecular clouds in this shell, so that their physical parameters can be derived. This shell is seen over the velocity range from  $-22 \text{ km s}^{-1}$  to  $-13 \text{ km s}^{-1}$  and does not show any velocity structure. The kinematic distance to the shell is 3.8 kpc (Heiles 1984). It is unlikely, however, that this is the actual distance to the clouds because then the molecular clouds are located at 1.9 kpc below the galactic plane and have masses greater than  $10^5 M_\odot$ ! There is an impression that the polarization vectors of stars in this area are lying parallel to the shell in the map of Mathewson and Ford (1970), in which case the shell is very close to us, i.e., less than 300 pc. Interstellar Ca II absorption lines had been measured for some of the stars in this area (see Habing 1969). HD 212097 ( $l = 87^\circ$ ,  $b = -24^\circ$ , distance = 80 pc) has no Ca II lines corresponding to the H I velocities of the shell. On the other hand, HD 215733 ( $l = 85^\circ$ ,  $b = -36^\circ$ , distance = 2.1 kpc) has a Ca II line at  $-17.4 \text{ km s}^{-1}$ . Another piece of information on the distance may be obtained by assuming that the observed H I mass ( $\sim \text{area} \times \text{column density}$ ) cannot be greater than the original mass in the volume inside the shell. Using a mean H I column density of  $5 \times 10^{19} \text{ cm}^{-2}$ , we get a lower limit of  $\sim 10(n_0/1 \text{ cm}^{-3}) \text{ pc}$ , where  $n_0$  is the initial density in this

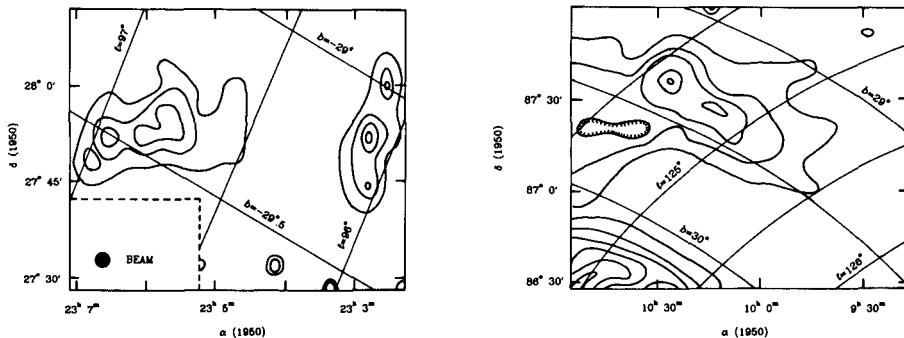


Figure 2. Maps of CO emission detected in two galactic H I shells, GS 090-28-17 and GS 135+29+4. The contour of velocity-integrated antenna temperature increases from  $1 \text{ K km s}^{-1}$  by increments of  $1 \text{ K km s}^{-1}$ .

region. Therefore, in summary, the clouds associated with the H I shell are probably located between 80 pc and 300 pc away from us. If we adopt a distance of 200 pc, the sizes ( $\sqrt{\text{area}/\pi}$ ) of two molecular clouds are 0.6 pc and 1.0 pc, respectively. The masses are  $80 M_{\odot}$  and  $340 M_{\odot}$  estimated from the ratio  $N_{\text{H}_2}/\int T_{\text{R}} dv = 0.5 \times 10^{20} \text{ cm}^{-2} (\text{K km s}^{-1})^{-1}$  obtained by de Vries et al. (1987) for the high latitude molecular clouds in Ursa Major.

Since they are physically associated with the H I shell, it is natural to consider them to be formed in the shell. (If they are pre-existing clouds, it is difficult to explain the coincidence of CO velocity with H I velocity.) There are at least two possible mechanisms for the formation of clouds in the shell: First mechanism is of course the gravitational instability. McCray and Kafatos (1987) developed a scenario such that clouds are formed inside H I shells by the onset of gravitational instability. However, unless the observed clouds are at a distance greater than  $\sim 2$  kpc, they are not gravitationally bound (we used velocity width of  $1 \text{ km s}^{-1}$ ). Alternatively, and more likely, the clouds could be formed by thermal instability in the radiative cooling region behind the shock front (e.g., McCray, et al. 1975). In this case, since the growth rate depends on  $\lambda/c\tau_c$  (Schwarz et al. 1972) where  $\lambda$  is the wavelength of perturbation,  $c$  is the sound speed of the gas, and  $\tau_c$  is the radiative cooling time, the clouds with different sizes and different masses will be formed depending upon the wavelength of the initial perturbations and the age of the shell.

## References

- de Vries, H. W., Heithausen, A., and Thaddeus, P. 1987, *Ap. J.*, in press.
- Habing, H. J. 1969, *Bull. Astr. Inst. Netherlands*, 20, 177.
- Heiles, C. 1976, *Ap. J. (Letters)*, 208, L137.
- Heiles, C. 1984, *Ap. J. Suppl.*, 55, 585.
- Heiles, C. and Habing, H. J. 1974, *Astr. Ap. Suppl.*, 14, 1.
- Mathewson, D. S. and Ford, V. L. 1970, *Mem.R.A.S.*, 74, 139.
- McCray, R. and Kafatos M. C. 1987, *Ap. J.*, 317, 190.
- McCray, R., Stein, R. F., and Kafatos M. C. 1975, *Ap. J.*, 196, 565.
- Schwarz, J., McCray, R., and Stein, R. F. 1972, *Ap. J.*, 175, 673.